Analysis of Ca^2 Response of Osteocyte Network by Three-dimensional Time-lapse Imaging in Living Bone

AUTHOR(S):

Tanaka, Tomoyo; Hoshijima, Mitsuhiro; Sunaga, Junko; Nishida, Takashi; Hashimoto, Mana; Odagaki, Naoya; Osumi, Ryuta; Adachi, Taiji; Kamioka, Hiroshi

CITATION:

Tanaka, Tomoyo ...[et al]. Analysis of Ca^2 Response of Osteocyte Network by Three-dimensional Time-lapse Imaging in Living Bone. Journal of Bone and Mineral Metabolism 2018, 36(5): 519-528

ISSUE DATE:

2018-09

URL:

http://hdl.handle.net/2433/235750

Analysis of Ca^{2+} response of osteocyte network by three-dimensional time-lapse imaging in living bone

Tomoyo Tanaka[1], Mitsuhiro Hoshijima[1,2], Junko Sunaga[3], Takashi Nishida[4], Mana Hashimoto[1], Naoya Odagaki[1], Ryuta Osumi[1], Taiji Aadachi[3], Hiroshi Kamioka[1*]

[1]Department of Orthodontics, Graduate School of Medicine, Dentistry and Pharmaceutical Sciences, Okayama University, Japan

[2]Advanced Research Center for Oral and Craniofacial Sciences, Dental School, Okayama University, Japan

[3]Laboratory of Biomechanics, Department of Biosystems Science, Institute for Frontier Life and Medical Sciences, Kyoto University, Japan

[4]Department of Biochemistry and Molecular Dentistry, Graduate School of Medicine, Dentistry and Pharmaceutical Sciences, Okayama University, Japan

*: Corresponding author

5-1 Shikata-cho, 2-chome, kitaku, Okayama 700-8525, Japan

Tel: 81-86-235-6690, Fax: 81-86-235-6694

e-mail: kamioka@md.okayama-u.ac.jp

Keywords: osteocyte, MLO-Y4, fluid shear stress, 3D time-lapse imaging

Abstract

Osteocytes form a three-dimensional (3D) cellular network within the mineralized bone matrix. The cellular network has important roles in mechanosensation and mechanotransduction related to bone homeostasis. We visualized embedded osteocytes network in chick calvariae and observed the flow-induced Ca^{2+} signaling in osteocytes using 3D time-lapse imaging. In response to the flow, intracellular Ca^{2+} ($[Ca^{2+}]_i$) significantly increased in developmentally mature osteocytes in comparison with young osteocytes in the bone matrix. To investigate the differences in response between young and developmentally mature osteocytes in detail, we evaluated the expression of osteocyte-related genes using the osteocyte-like cell line MLO-Y4, which was 3D-cultured within type I collagen gels. We found that the *c-Fos*, *Cx43*, *Panx3*, *Col1a1* and *OCN* mRNA levels significantly increased on Day 15 in comparison with Day 7. These findings indicate that developmentally mature osteocytes are more responsive to mechanical stress than young osteocytes, and play important roles in bone formation and remodeling.

Introduction

Osteocytes form a three-dimensional (3D) cellular network within the mineralized bone matrix, and long dendrites of osteocytes interact with not only neighboring osteocytes but also osteoblasts on the bone surface [1, 2]. The osteocyte network functions as a mechanosensory system, translating mechanical stimuli into electrical or biochemical signals and organizing osteoblasts and osteoclasts to perform bone formation and resorption [3-8].

Various mechanical stimuli have been shown to act through numerous signaling pathways to promote bone cell activity *in vitro* [9-11]. Fluid shear stress increases $[Ca^{2+}]_i$ by enhanced entry through mechanosensitive ion channels [12]. This $[Ca^{2+}]_i$ increase may act as a secondary messenger and mediate the activity of intracellular signal transduction [13]. Previous studies have reported that fluid shear stress induced rapid transient increases $[Ca^{2+}]_i$ in isolated bone cells *in vitro* [14-16]. Furthermore, fluid shear stress was specifically delivered to the bone surface and enhanced the activation of the autonomous $[Ca^{2+}]_i$ oscillations in osteoblasts and osteocytes via gap junction-mediated cell-cell communications and hemichannels [17].

Connexin 43 (Cx43) is a major gap junction protein and plays important roles in bone growth and remodeling [18, 19]. Mechanical loading induces the opening of the Cx43 hemichannels involved in communicating with the extracellular environment [20, 21]. Furthermore, the Pannexin 3 (Panx3) endoplasmic reticulum (ER) Ca^{2+} channel increases

$[Ca^{2+}]_i$ levels, which leads to activation of the calmodulin (CaM) kinase pathway and functions to switch the chondrocyte cell fate [22, 23]. However, the molecular mechanisms of their channels by which osteocytes regulate bone formation and remodeling in the 3D environment are poorly understood.

In the 3D cellular network, developmentally mature osteocytes in calcified area are embedded throughout the mineralized matrix, whereas the cells surrounded by the not-yet-completely mineralized bone matrix are osteoid, young osteocytes [24]. The increase in the $[Ca^{2+}]_i$ by mechanical stress was correlated with the enhancement of the c-Fos expression via cell-cell communication through gap junctions [17, 25]. In order to investigate the electrical or biochemical signals for 3D-networked osteocytes that may be involved in the regulatory functions of bone formation and remodeling, we evaluated the different patterns of the fluid shear stress-induced $[Ca^{2+}]_i$ distribution between young and developmentally mature osteocytes in chick calvariae using 3D time-lapse imaging.

However, isolated osteocytes cultured on a dish do not behave as they would *in vivo* in a 3D complex [25], which has made it difficult to study their molecular mechanisms in response to $[Ca^{2+}]_i$ signaling in intact osteocytes. To mimic an *in vivo* environment, the mouse osteocyte-like cell line MLO-Y4 was 3D-cultured in collagen gel [26, 27], and the expression levels of osteocyte-related genes were evaluated to determine the differences between young and developmentally mature osteocytes *in vitro*.

In this study, we show for the first time that $[Ca^{2+}]_i$ drastically increased in developmentally mature osteocytes in comparison with young osteocytes in response to fluid shear stress *ex vivo*. We further show that *c-Fos*, *Cx43*, *Panx3*, *Col1a1* and *Osteocalcin* (*OCN*) mRNA expression was induced in the mature MLO-Y4 cells 3D-cultured for a long time.

Materials and Methods

Preparation of bone fragments

Bone fragments were prepared from 16-day-old chick embryonic calvariae. The calvariae were washed with alpha-modified Minimum Essential Medium (α-MEM; Invitrogen, Carlsbad, CA, USA) to remove non-adherent cells. After stripping off the periosteum, the samples were trimmed into 3×5-mm pieces for further use.

Multiphoton laser scanning imaging and differential interference imaging

The osteocytes in the chick calvariae were visualized with a FLUOVIEW FV1200 MPE microscopy system (Olympus, Tokyo, Japan) equipped for differential interference contrast (DIC) microscopy. A multiphoton laser scanning microscope (MPLSM) was coupled to an upright microscope (IX83; Olympus) with a ×60 (NA = 1.4) oil-immersion objective lens.

Induction of fluid shear stress

Bone samples were placed on cover slips (MATSUNAMI, Osaka, Japan) and held in a flow

chamber using adhesive grease. Capillary diffusion-aided fluid flow was applied to the samples by adding a drop of medium to one side of the slide glass and sucking the solution from the opposite side using a 1-ml syringe (Fig.1a). We used α-MEM as the flow solution. 1-ml syringe was set in a programmable syringe pump (KD-Scientific, Holliston, MA, USA) which sucked a solution at a rate of 0.1 ml/min.

Dye loading and calcium imaging

The intracellular calcium concentration was measured using a calcium indicator probe, Fluo-8 No Wash (Fluo-8 NW) Calcium Assay Kit (AAT Bioquest, Inc. Sunnyvale, CA, USA). Individual cultures were incubated for 20 min at 37°C in Hanks' buffer with 20 mM Hepes (HHBS) containing 10 μM Fluo-8 NW dissolved in dimethyl sulfoxide (DMSO) and 10% Pluronic F-127. The chick calvariae were rinsed with flow medium, and cover slips were affixed to the flow chamber and mounted on the MPLSM system. The scanning rate was 1.23 s/frame for 16-bit images 512×512 pixels in size. The frame size of the images was 212×212 μm. Multiphoton images were taken with a 2.5-μm step size. The settings for PMT, gain, and offset were fixed in all experiments. Time-lapsed images were recorded every 11.1 s, starting 323.2 s prior to the application of the fluid flow stress for recording baseline intensity before loading. The $[Ca^{2+}]_i$ was analyzed as the average intensity of the fluorescence using an excitation wavelength of 830 nm. The total imaging and loading period was 657.6 s (540 scans

without an interval). We used 10 μM Fura Red AM (Invitrogen) as a ratiometric Ca^{2+} imaging dye to avoid time-dependent loss of signal [17, 25, 28].

Cell culture

The MLO-Y4 cell line is a murine long bone-derived model of an osteocyte [24]. MLO-Y4 cells were cultured on collagen-coated plates in α-MEM supplemented with 10% fetal bovine serum (FBS) and 1% penicillin-streptomycin (P/S) in 5% CO_2 at 37°C. The medium was changed twice a week, and the cells were passaged after they reached 70% to 80% confluency.

3D cell culture

MLO-Y4 cells were incorporated within type I collagen gels. Porcine tendon type I collagen (Nitta Gelatin, Osaka, Japan) was mixed at 1:1 with 2×α-MEM. MLO-Y4 cells (1.5×10^6 cells/mL gel) diluted in α-MEM, including the gel, were distributed into 12-well plastic plates by 1 ml, respectively, and polymerized at 37°C for 20 min. α-MEM with 10% FBS were applied onto the surface of each gel after 20 min and incubated at 37°C. The medium was changed every 2 or 3 days thereafter.

Morphological analysis of osteocytes and MLO-Y4 cells

The samples of chick calvariae were fixed with 4% paraformaldehyde in PBS for 10 min. After

several rinses with PBS, chick calvariae were stained with Alexa 488 Phalloidin (diluted 1:40, Invitrogen) to stain the actin cytoskeleton and DAPI (diluted 1:500, Invitrogen) to stain the nucleus for 60 min. The fixation and the staining were all carried out at room temperature. The fluorescent images were acquired using a FLUOVIEW FV500 confocal laser scanning microscopy (Olympus). The length of osteocytes processes and MLO-Y4 cells were measured using NIH ImageJ software, as reported previously [29].

mRNA extraction, RT-PCR, and qRT-PCR

Total RNA of MLO-Y4 cells was extracted using an RNeasy Mini Kit (Quiagen, Hilden, Germany) in accordance with the manufacturer's instructions. For quantification of mRNA expression, 0.5 μg of total RNA of each sample was reverse-transcribed with avian myeloblastosis virus (AMV) reverse transcriptase (Takara Bio, Shiga, Japan) at 37°C for 15 min. Quantitative real-time polymerase chain reaction (qRT-PCR) using SYBR Green Realtime PCR Master Mix (Toyobo, Osaka, Japan) was done with StepOnePlus (Applied Biosystems, Foster City, USA). All primer sequences are reported in Table 1, and the mRNA expression was normalized to the expression of the housekeeping gene *Gapdh*.

Results

3D time-lapse imaging of $[Ca^{2+}]_i$ signaling in osteocytes via MPLSM.

To monitor the 3D $[Ca^{2+}]_i$ signaling of osteocytes in intact bone samples, embryonic chick

calvariae were loaded with Fluo-8 NW to be observed with the MPLSM system (Fig. 1a). The 3D reconstruction of the osteocyte network using the Volocity software program (Perkin Elmer, Kanagawa, Japan) was performed using multiphoton images from 0 to 20 μm in depth (Fig. 1b). The 3D time-lapse data showed that some osteocytes displayed autonomous $[Ca^{2+}]_i$ oscillation under static conditions, and fluid flow induced a $[Ca^{2+}]_i$ response. Twelve cells were randomly selected in the bone, and the average value of the fluorescence intensity, after excluding the maximum and minimum values, was calculated at a certain point in time before and after the fluid flow.

Analyzing the effects of mechanical stress on the $[Ca^{2+}]_i$ response in young and developmentally mature osteocytes.

Osteoid bone was identified using DIC images, as reported previously [2]. Polygonal osteoblasts covered the surface of the calvariae, and the external appearance of the calcified area was examined under the osteoblast layer using DIC images. Deeper into the calvariae, DIC images showed decreased number of the osteoblasts and appeared young osteocytes, surrounded by incompletely mineralized bone matrix. Developmentally mature osteocytes located in lacunae surrounded by mineralized bone matrix has been seen 20 μm below the osteoblast layer by the DIC and MPLSM. 0-20 μm below the osteoblast layer, lacunae were unclear in bone matrix, because there is not completely mineralized and osteocytes were not

embedded bone matrix. In this study, we defined calcified area was 20 μm below from the osteoblast layer and osteoid bone was between osteoblast layer and calcified area. We then evaluated the $[Ca^{2+}]_i$ changes in individual osteocytes fluorescently labeled with Fluo-8 NW. The fluorescently labeled young osteocytes in osteoid were able to be observed 12.5 μm below the bone surface (Fig. 2a, b), and developmentally mature osteocytes in calcified area were able to be observed more than 7.5 μm (Fig. 2c, d). To analyze the effects of mechanical stress on the $[Ca^{2+}]_i$ response, fluid shear stress was applied to the calvariae.

The means of the fluorescence ratio measured in individual osteocytes in calcified area and osteoid area are represented as the time courses (Fig. 2e). Upon the initiation of flow-induced mechanical stress, the individual osteocytes responded with a sudden increase in the $[Ca^{2+}]_i$ of developmentally mature osteocytes in calcified area (Fig. 2c, d arrows, n=10). In contrast, the $[Ca^{2+}]_i$ of young osteocytes was not significantly increased by flow-induced mechanical stress (n=10) (Fig. 2f).

Morphological characteristics of young and developmentally mature osteocytes in vivo

We next observed the localization and morphology of osteocytes in the chick calvariae. The dashed line in the DIC image shows the outline of the osteoid and calcified area (Fig. 3a, c). In calcified area, the osteocytes were more spindle-shaped than in osteoid, and the long axes of the osteocytes were aligned parallel to the longitudinal axes of the trabecula. Furthermore, the

osteocytes in calcified area showed more processes than those in the osteoid, and the process contacts between neighboring osteocytes were revealed by actin filament staining (Fig. 3b, d). Average individual dendrite length of osteocytes within the matrices was 7.93 μm in osteoid and 10.3 μm in calcified area. There was significant difference in the individual dendrite length of osteocytes in osteoid and calcified area (Fig. 3e).

Characteristics of MLO-Y4 cells in 3D culture

To observe the morphological changes in the osteocytes in an environment mimicking the intact bone, MLO-Y4 cells were incorporated into type I collagen gels. After 3 days, the cells were small with short processes (Fig. 4a). After 7 days, these processes became elongated and continued to make contact with other cells (Fig. 4b, d). MLO-Y4 cells at 3 to 7 days of culture showed structures similar to those of “young osteocytes” in the osteoid (Fig. 3b, Fig. 4a, b). The MLO-Y4 cells at Day15 had formed longer processes, their projections extended in three dimensions, and the dendritic morphology of the observed cells was similar to that of the “developmentally mature osteocytes” in calcified area (Fig. 3d, Fig. 4c). Furthermore, average individual dendrite length of the MLO-Y4 cells in 3D culture matrices was 18.9 μm at Day 3, 21.4 μm at Day 7 and 24.7 μm at Day 15, the difference of dendrite length between young oseteocytes and developmentally mature osteocytes was statistically significant (Fig.4d).

Dmp1 and *Sost* are characteristic osteocyte marker genes [30]. The expression of

osteocytic markers in the 3D cultures over time was analyzed by qRT-PCR. Within the 3D cultures, *Sost* mRNA reached its maximum expression at Day 15, while the *Dmp1* mRNA expression was highest at Day 7 (Fig. 4e, f). These results indicate that, for the first 7 days, MLO-Y4 cells in the 3D cultures mimicked osteoblastic, osteoid, young osteocytes of the facial bone layer, but the cells at 10 to 15 days were similar to mature osteocytes distributed over the inside of the bone.

Gene expression in 3D-cultured MLO-Y4 cells

MLO-Y4 cells will likely prove a useful model for studying not only the differentiation process but also the gene expression of osteocytes [26]. To elucidate the relationship between Ca^{2+} signaling and the gene expression in osteocytes, we subsequently investigated the differences in the *Fgf23*, *c-Fos*, *Cx43*, *Panx3*, *Col1a1* and *OCN* mRNA expression between young osteocytes on Day 7 and mature osteocytes on Day 15 using 3D-cultured MLO-Y4 cells (Fig. 5a-f). In the MLO-Y4 cells on Day 15, *c-Fos*, *Cx43*, *Col1a1* and *OCN* mRNA expression were significantly increased in comparison with that on Day 7 (Fig. 5b-f). There was no marked difference in the mRNA levels of *Fgf23* (Fig. 5a). These data suggest that the increase in expression level of channel-related genes is enhanced the potential of the Ca^{2+} responses in developmentally mature osteocytes, similarly, promoting the expression of mineralization-related genes such as *Col1a1* and *OCN* compared with the expression in young osteocytes.

Discussion

Time-lapse images of $[Ca^{2+}]_i$ signaling of osteoblasts and osteocytes in previous reports have shown only single optical slices for each layer [17, 25, 31, 32]. However, it is not entirely clear how the $[Ca^{2+}]_i$ responses are produced in a 3D cellular network. Conventional fluorescence live imaging has been limited by phototoxity and photobleaching [33]. Therefore, in this study, we used 3D-time lapse imaging to analyze the real-time $[Ca^{2+}]_i$ signaling in osteocytes in intact bone explants. $[Ca^{2+}]_i$ signaling of osteocytes embedded in mineralized bone matrix was observed using an MPLSM, which has advantages for resolving these problems. Furthermore, our method allowed for the analysis of $[Ca^{2+}]_i$ signaling in young and developmentally mature osteocytes within the same living bone samples under the same conditions. Our 3D time-lapse imaging and analysis provided insights into osteocyte Ca^{2+} mechanotransduction via cell-cell communication at the organ level.

According to previous reports, fluid flow-induced $[Ca^{2+}]_i$ response was measured in isolated cells and *ex vivo* because the fluid flow through the lacuno-canalicular system induces shear stress to the bone explant [17]. The bone is a complex tissue composed of an organic matrix, predominately collagen, and the osteocytes are embedded in the mineralized matrix. We therefore suggest that sensitivity to mechanical stimuli in osteocytes differs depending on the degree of maturity, calcification and environment. In the present study, we showed for the first time that $[Ca^{2+}]_i$ levels were significantly increased in developmentally mature osteocytes

in comparison with young osteocytes by flow-induced mechanical stress (Fig. 2a-f). These results indicate that the networks of mature osteocytes in calcified area are more responsive than those of young osteocytes in osteoid and under fluid flow stress. However, the gene expression in response to the $[Ca^{2+}]_i$ signaling between these two phenotypes has hardly been evaluated because of difficulties in accessing and characterizing osteocytes deeply embedded within hard bone structures *in vivo* and *ex vivo* [34]. Consequently, using a model that closely mimics the young and developmentally mature osteocytes *in vivo* for the analysis of gene expression will prove useful.

In 3D culture models, MLO-Y4 cells display dendritic morphology that allows communication with neighboring cells [35, 36]. In the previous study, Sugawara et al. showed the morphological changes in the osteocytes during normal growth and compared the formation of the 3D osteocyte network in the presence and absence of mechanical loading [37]. We also compared the morphology of young and developmentally mature osteocytes by staining for actin filaments with phalloidin-conjugated fluorescence. In the calcified area, the mature osteocytes were more spindle-shaped, and the processes were longer than in the young osteocytes in the osteoid (Fig. 3b, d, e). In the 3D-cultured MLO-Y4 cells observed after 7 days, the morphological phenotype formed within type I collagen gels seemed to resemble the physiological process that occurs when young osteocytes develop in newly formed osteoid (Fig. 4b). MLO-Y4 cells maintained until Day 15 in the 3D culture were similar to the

developmentally mature osteocytes that formed longer processes in calcified area (Fig. 4c, d). Previous studies have shown that *Dmp1* expression was observed in young osteocytes of the superficial bone layer but was reduced remarkably in old osteocytes [38], and DMP1 expression in the extracellular matrix is required for the downregulation of osteoblast markers and normal osteocyte differentiation [39]. The expression pattern of *Sost* remains consistent in the mineralized tissues during both development and in adult bone [40]. In this study, the upregulation of *Sost* mRNA as a mature osteocytic marker observed at Days 7 to 10 and the time-dependent decrease in the *Dmp1* mRNA expression in 3D culture were characteristic of the osteocyte gene expression profile (Fig. 4e, f). Furthermore, the increases in the $[Ca^{2+}]_i$ by fluid flow stress were coupled with increases in the *c-fos* mRNA expression in the explants [17]. Wang et al. comprehensively quantified the gap junctional intercellular communication capacity in embryonic chick calvariae and indicated that the cell-cell communication capacity of the osteocytes was related to their development [41]. Our studies in 3D-culture with MLO-Y4 cells also indicate that there are differences in the expression of osteocyte-related genes between young osteocytes and developmentally mature osteocytes (Fig. 5b, c). These suggest that, under appropriate conditions, the MLO-Y4 cells within the 3D culture may develop from young osteocytes into mature osteocytes.

To assess the difference in the physiological function of these two phenotypes, we then compared the gene expression after 7 days' culture with the levels at Day 15 in this 3D system.

We found that *Panx3* mRNA levels were increased at Day 15 in the cultured MLO-Y4 cells (Fig. 5d). The pannexin family has three members and participates in ER Ca^{2+} leakage and $[Ca^{2+}]_i$ movement [42]. Panx3 show the high levels expression in developing hard tissues, including cartilage and bone whereas Panx1 and 2 are preferentially expressed in the central nervous system [22, 23]. This result regarding the enhancement of *Panx3* mRNA expression at Day 15 of culture are consistent with the drastic increase in $[Ca^{2+}]_i$ in the mature osteocytes within calcified area. Furthermore, the *Col1a1* and *OCN* mRNA expression was higher at Day 15 than in 7-day 3D cultures, suggesting that developmentally mature osteocytes have greater potential for mechanically induced bone formation and remodeling than younger osteocytes (Fig. 6). Fgf23 may play a role in a later phase of development than collagen type I and osteocalcin [34]. These findings suggest, than when young osteocytes develop into mature osteocytes, the $[Ca^{2+}]_i$ responses are drastically enhanced by mechanical stimuli. Therefore, the mature osteocytes at a deep location within bone may strongly promote bone formation and remodeling.

Acknowledgments

This work was performed in part under the Cooperative Research Program of Institute for Frontier Medical Sciences, Kyoto University, Japan and supported by a Grant-in-Aid for Scientific Research (no. JP 16H05549) from the Ministry of Education, Culture, Sports,

Science and Technology (MEXT), Japan.

Conflict of interest

All authors have no conflicts of interest.

References

1. Power J, Loveridge N, Rushton N, Parker M, Reeve J (2002) Osteocyte density in aging subjects is enhanced in bone adjacent to remodeling haversian systems. Bone 30:859-865.
2. Kamioka H, Honjo T, Takano-Yamamoto T (2001) A three-dimensional distribution of osteocyte processes revealed by the combination of confocal laser scanning microscopy and differential interference contrast microscopy. Bone 28:145-149.
3. Gu G, Kurata K, Chen Z, Väänänen KH (2007) Osteocyte: a cellular basis for mechanotransduction in bone. Journal of Biomechanical Science and Engineering 2**:**150-165.
4. Hu M, Tian GW, Gibbons DE, Jiao J, Qin YX (2015) Dynamic fluid flow induced mechanobiological modulation of in situ osteocyte calcium oscillations. Arch Biochem Biophys 579:55-61.
5. Bonewald LF, Johnson ML (2008) Osteocytes, mechanosensing and Wnt signaling. Bone 42:606-615.
6. Klein-Nulend J, Bakker AD, Bacabac RG, Vatsa A, Weinbaum S (2013) Mechanosensation and transduction in osteocytes. Bone 54:182-190.
7. Komori T (2013) Functions of the osteocyte network in the regulation of bone mass. Cell Tissue Res 352:191-198.

8. Bonewald LF (2006) Mechanosensation and transduction in osteocytes. Bonekey Osteovision 3:7-15.

9. Hughes-Fulford M (2004) Signal transduction and mechanical stress. Sci STKE

10. Wadhwa S, Godwin SL, Peterson DR, Epstein MA, Raisz LG, Pilbeam CC (2002) Fluid flow induction of cyclo-oxygenase 2 gene expression in osteoblasts is dependent on an extracellular signal-regulated kinase signaling pathway. J Bone Miner Res 17:266-274.

11. Wadhwa S, Choudhary S, Voznesensky M, Epstein M, Raisz L, Pilbeam C (2002) Fluid flow induces COX-2 expression in MC3T3-E1 osteoblasts via a PKA signaling pathway. Biochem Biophys. Res Commun 297:46-51.

12. You J, Reilly GC, Zhen X, Yellowley CE, Chen Q, Donahue HJ, Jacobs CR (2001) Osteopontin gene regulation by oscillatory fluid flow via intracellular calcium mobilization and activation of mitogen-activated protein kinase in MC3T3-E1 osteoblasts. J Biol Chem 276:13365-71.

13. Berridge MJ, Bootman MD, Lipp P (1998), Calcium-a life and death signal. Nature 395: 645-648.

14. Kamioka H, Sugawara Y, Murshid SA, Ishihara Y, Honjo T, Takano-Yamamoto T (2006) Fluid shear stress induces less calcium response in a single primary osteocyte than in a single osteoblast: implication of different focal adhesion formation. J Bone Miner Res 21:1012-1021.

15. Lu XL, Huo B, Chiang V, Guo XE (2012) Osteocytic network is more responsive in calcium signaling than osteoblastic network under fluid flow. J Bone Miner Res 27:563-574.

16. Hung CT, Pollack SR, Reilly TM, Brighton CT (1995) Real-time calcium response of cultured bone cells to fluid flow. Clin Orthop Relat Res:256-269.

17. Ishihara Y, Sugawara Y, Kamioka H, Kawanabe N, Hayano S, Balam TA, Naruse K, Yamashiro T (2013) Ex vivo real-time observation of Ca^{2+} signaling in living bone in response to shear stress applied on the bone surface. Bone 53:204-215.

18. Xu H, Gu S, Riquelme MA, Burra S, Callaway D, Cheng H, Guda T, Schmitz J, Fajardo RJ, Werner SL, Zhao H, Shang P, Johnson ML, Bonewald LF, Jiang JX (2015) Connexin 43 channels are essential for normal bone structure and osteocyte viability. J Bone Miner Res 30:436-448.

19. Ilvesaro J, Väänänen K, Tuukkanen J (2000) Bone-resorbing osteoclasts contain gap-junctional connexin-43. J Bone Miner Res. 15:919-926.

20. Burra S, Nicolella DP, Francis WL, Freitas CJ, Mueschke NJ, Poole K, Jiang JX (2010), Dendritic processes of osteocytes are mechanotransducers that induce the opening of hemichannels. Proc. Natl Acad Sci USA 107:13648-13653.

21. Cherian PP, Siller-Jackson AJ, Gu S, Wang X, Bonewald LF, Sprague E, Jiang JX (2005) Mechanical strain opens connexin 43 hemichannels in osteocytes: a novel mechanism for

the release of prostaglandin. Mol Biol Cell 16:3100-3106.

22. Iwamoto T, Nakamura T, Doyle A, Ishikawa M, de Vega S, Fukumoto S, Yamada Y (2010) Pannexin 3 regulates intracellular ATP/cAMP levels and promotes chondrocyte differentiation. J Biol Chem. 285:18948-18958.

23. Ishikawa M, Iwamoto T, Fukumoto S, Yamada Y(2014) Pannexin 3 inhibits proliferation of osteoprogenitor cells by regulating Wnt and p21 signaling. J Biol Chem. 289:2839-2851.

24. Palumbo C (1986) A three-dimensional ultrastructural study of osteoid-osteocytes in the tibia of chick embryos. Cell Tissue Res 246:125-131.

25. Ishihara Y, Sugawara Y, Kamioka H, Kawanabe N, Kurosaka H, Naruse K, Yamashiro T (2012) In situ imaging of the autonomous intracellular Ca^{2+} oscillations of osteoblasts and osteocytes in bone. Bone 50:842-852.

26. Kato Y, Windle JJ, Koop BA, Mundy GR, Bonewald LF (1997) Establishment of an osteocyte-like cell line, MLO-Y4. J Bone Miner Res 12:2014-2023.

27. Kurata K, Heino TJ, Higaki H, Väänänen HK (2006) Bone marrow cell differentiation induced by mechanically damaged osteocytes in 3D gel-embedded culture. J Bone Miner Res 21:616-625.

28. Adachi T, Aonuma Y, Tanaka M, Hojo M, Takano-Yamamoto T, Kamioka H (2009) Calcium response in single osteocytes to locally applied mechanical stimulus: differences in cell process and cell body. J Biomech 42:1989-1995.

29. Mc Garrigle MJ, Mullen CA, Haugh MG, Voisin MC, McNamara LM (2016) Osteocyte differentiation and the formation of an interconnected cellular network in vitro. Eur Cell Mater 31:323-40.

30. Noble BS (2008) The osteocyte lineage. Arch Biochem Biophys 2:106–111.

31. Jing D, Baik AD, Lu XL, Zhou B, Lai X, Wang L, Luo E, Guo XE (2014) In situ intracellular calcium oscillations in osteocytes in intact mouse long bones under dynamic mechanical loading. FASEB J 28:1582-1592.

32. Adachi T, Aonuma Y, Ito S, Tanaka M, Hojo M, Takano-Yamamoto T, Kamioka H (2009) Osteocyte calcium signaling response to bone matrix deformation. J Biomech 42:2507-2512.

33. Hoebe RA, Van Oven CH, Gadella TWJ, Dhonukshe PB, Van Noorden CJF, Manders EMM (2007) Controlled light-exposure microscopy reduces photobleaching and phototoxicity in fluorescence live-cell imaging. Nat Biotechnol 25:249-253.

34. Woo SM, Rosser J, Dusevich V, Kalajzic I, Bonewald LF (2011), Cell line IDG-SW3 replicates osteoblast-to-late-osteocyte differentiation in vitro and accelerates bone formation in vivo. J Bone Miner Res 26:2634-2646.

35. Vazquez M, Evans BA, Riccardi D, Evans SL, Ralphs JR, Dillingham CM, Mason DJ (2014) A new method to investigate how mechanical loading of osteocytes controls osteoblasts. Front Endocrinol (Lausanne) 5:208.

36. Boukhechba F, Balaguer T, Michiels JF, Ackermann K, Quincey D, Bouler JM, Pyerin W, Carle GF, Rochet N (2009) Human primary osteocyte differentiation in a 3D culture system. J Bone Miner Res 24:1927-1935.

37. Sugawara Y, Kamioka H, Ishihara Y, Fujisawa N, Kawanabe N, Yamashiro T (2013) The early mouse 3D osteocyte network in the presence and absence of mechanical loading. Bone 52:189-196.

38. Toyosawa S, Oya K, Sato S, Ishida K (2012) Osteocyte and DMP1. Clin Calcium 22:713-720.

39. Schiavi SC (2006) Bone talk. Nat Genet 38:1230-1231.

40. Atkins GJ, Rowe PS, Lim HP, Welldon KJ, Ormsby R, Wijenayaka AR, Zelenchuk L, Evdokiou A, Findlay DM (2011) Sclerostin is a locally acting regulator of late-osteoblast/preosteocyte differentiation and regulates mineralization through a MEPE-ASARM-dependent mechanism. J Bone Miner Res 26:1425-1436.

41. Wang Z, Odagaki N, Tanaka T, Hashimoto M, Nakamura M, Hayano S, Ishihara Y, Kawanabe N, Kamioka H (2016) Alternation in the gap-junctional intercellular communication capacity during the maturation of osteocytes in the embryonic chick calvaria. Bone 91:20-29.

42. Vanden AF, Bidaux G, Gordienko D, Beck B, Panchin YV, Baranova AV, Ivanov DV, Skryma R, Prevarskaya N (2006) Functional implications of calcium permeability of the

channel formed by pannexin 1. J Cell Biol. 174:535–546.

Figure legends

Fig. 1. Fluid shear stress application to calvariae and 3D time-lapse imaging of the autonomous and flow-induced $[Ca^{2+}]_i$ response in bone cells of intact calvariae. A schematic representation of the fluid flow device for 3D time-lapse imaging (a). The 3D reconstruction of the osteocyte network using the Volocity software program was performed with multiphoton images from 0 to 20 μm in depth (b).

Fig. 2. The time-lapse images showed the autonomous and flow-induced $[Ca^{2+}]_i$ response in osteocytes fluorescently labeled with Fluo-8 NW. Fluorescent and DIC images of the osteoid layer (a, b) were taken 12.5 μm below the chick calvariae surface, and those of the calcified layer (c, d) were taken 20 μm below the osteoblast layer (a, c were observed before mechanical loading, and b, d were observed after mechanical loading). The time course of the average fluorescence ratio, measured in individual osteocytes in calcified area and osteoid, was obtained every 11.1 s. The initiation of the flow-induced mechanical stress is indicated by the red arrow. The solid line represents the time course of the $[Ca^{2+}]_i$ response in developmentally mature osteocytes in calcified area, and the dashed line indicates that young osteocytes in osteoid (e). The red arrows showed the osteocytes increased $[Ca^{2+}]_i$ (c, d).The effect of fluid shear stress on the magnitude of the $[Ca^{2+}]_i$ increment observed in young osteocytes and developmentally mature osteocytes in intact bone (f). The data are expressed as the means ±

SD. The asterisks indicate a significant difference (*) (t-test $^{**}P < 0.01$).

Fig. 3. DIC and confocal images of actin and nuclei in osteocytes double-labeled and fluorescence stained with Alexa488 phalloidin and DAPI. The dashed line in the DIC images shows the outline of osteoid and trabecula (a, c). Superimposed images display osteocyte cell bodies stained with phalloidin (green) and their nuclei (blue) in osteoid layer (b) and calcified layer (d). (Bar=20 μm) Morphological data of average osteocyte dendrite length (e). The data are expressed as the means ± SD. The asterisks indicate a significant difference (t-test $^{**}P < 0.01$).

Fig. 4. Characterization of MLO-Y4 cells in 3D culture. MLO-Y4 cells were incorporated into type I collagen gels for 3 days (a), 7 days (b) and 15 days (c). Morphological data of average dendrite length of MLO-Y4 cells (d). The gene expression levels of *Sost* (e) and *Dmp1* (f) were analyzed over time by qRT-PCR. The data are expressed as the means ± SD of three independent samples of duplicate examinations. The asterisks indicate a significant difference (t-test $^{*}P < 0.05$, $^{**}P < 0.01$, $^{***}P < 0.001$).

Fig. 5. The gene expression profiles during maturation were compared at days 7 and 15 in 3D-cultured MLO-Y4 cells. qRT-PCR was performed to detect changes in the *Fgf23* (a), *c-Fos* (b),

Cx43 (c), *Panx3* (d), *Col1a1* (e) and *OCN* expression (f) relative to *Gapdh*. Each treatment was performed in duplicate, and the data represents three independent experiments (mean ± SD). ***p<0.001 relative to Day 7.

Fig. 6. Schematic diagram and characteristics of the young osteocyte as compared with developmentally mature osteocyte. The $[Ca^{2+}]_i$ responses in the developmentally mature osteocyte are strongly promoted by fluid flow stress. Therefore, the mature osteocytes at a deep location within bone may strongly promote the expression of mineralization-related genes such as *Col1a1* and *OCN* compared with the expression in young osteocytes.

Table 1. Primer sequences for mouse-derived cell line MLO-Y4

Gene (mouse)	Forward	Reverse
Sost	ggaatgatgccacagaggtcat	cccggttcatggtctggtt
Dmp1	agatcccctcttcgagaacttcgct	ttctgatgactcactgttcgtgggtg
Fgf23	gatccccacctcagttctca	ccggataggctctagcagtg
c-Fos	ccagtcaagagcatcagcaa	aagtagtgcagcccggagta
Cx43	ctcacctatgtctcctcct	ctggcttgcttgttgtaat
Panx3	gcccctggataagatggtcaag	gcggatggaacggttgtaaga
Col1a1	gagcggagagtactggatcg	tactcgaacgggaatccatc
OCN	gagtctgacaaagccttca	agccatactggtctgatag
Gapdh	caatgacccttcattgacc	gacaagcttcccgttctcag

Table 1

a

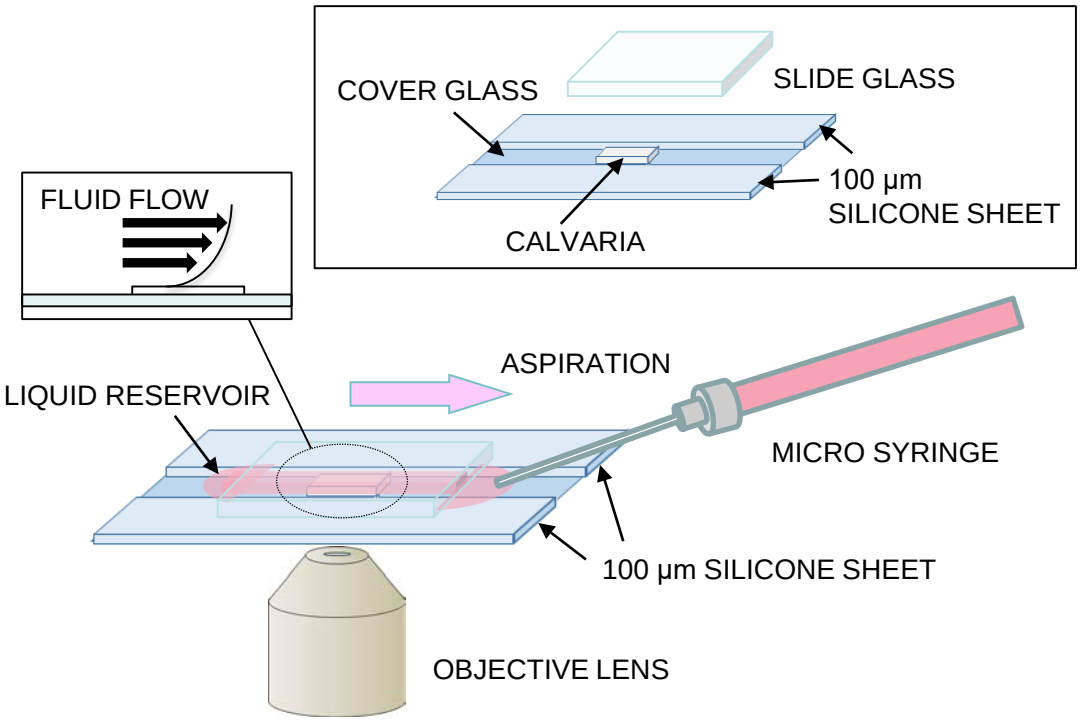

b

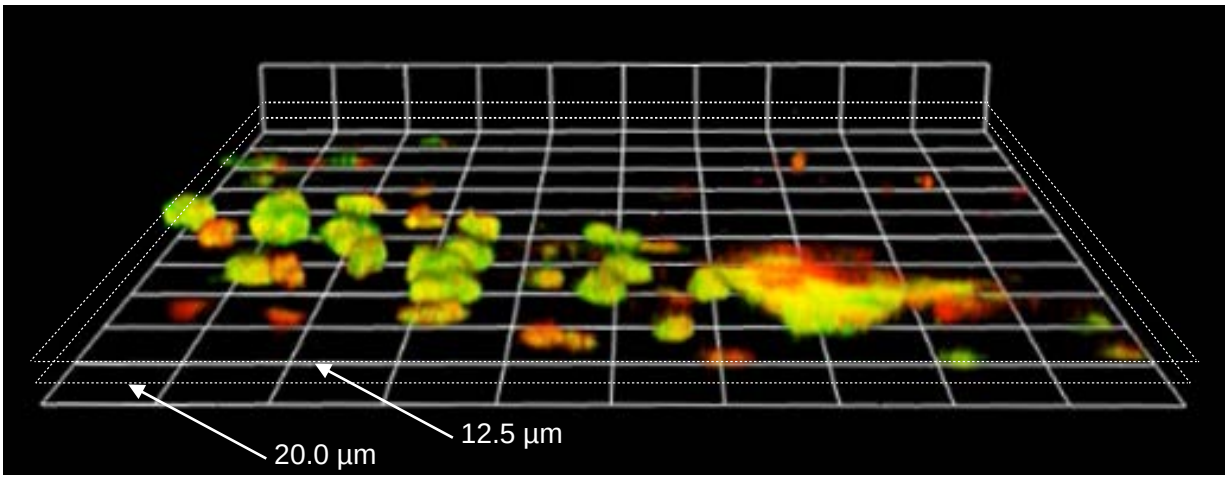

Fig. 1

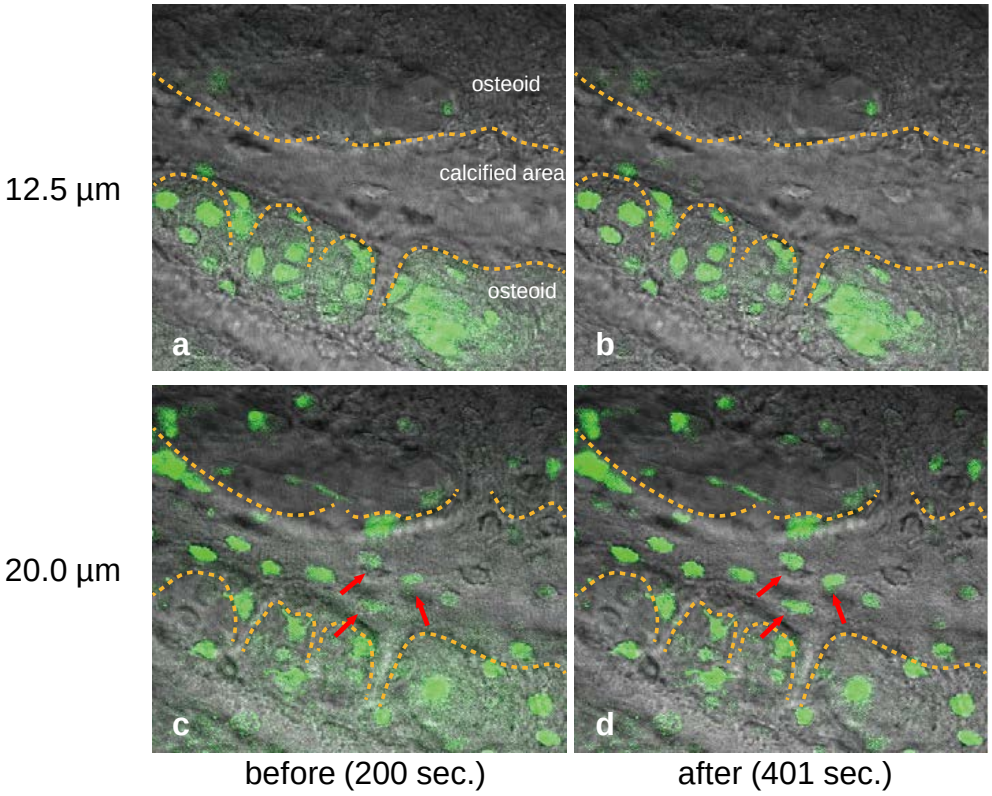

Fig. 2

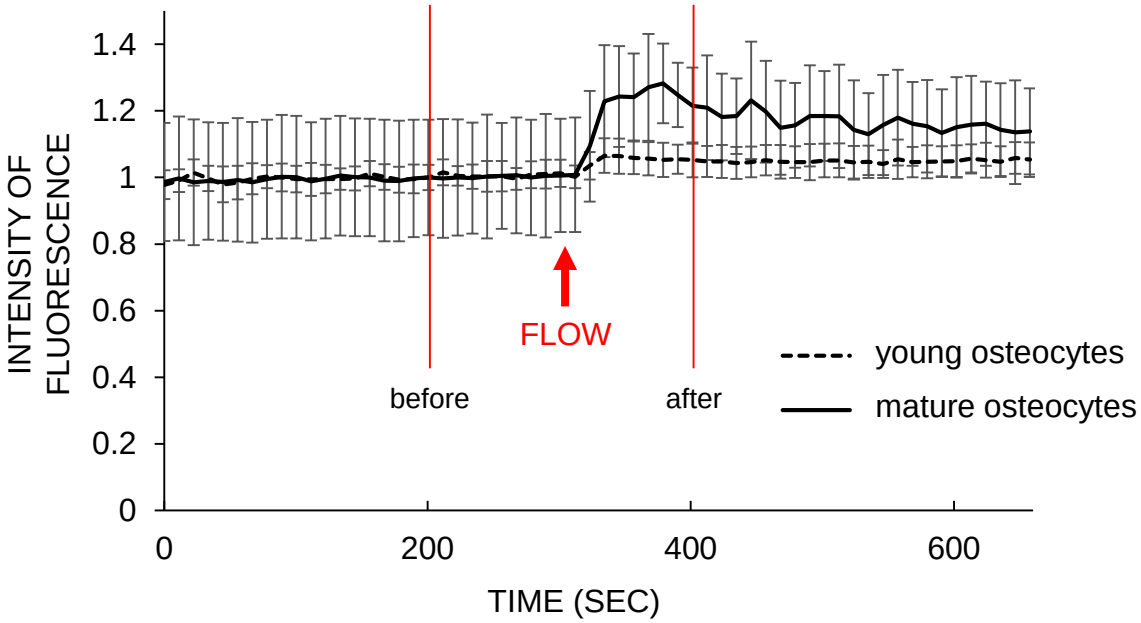

f

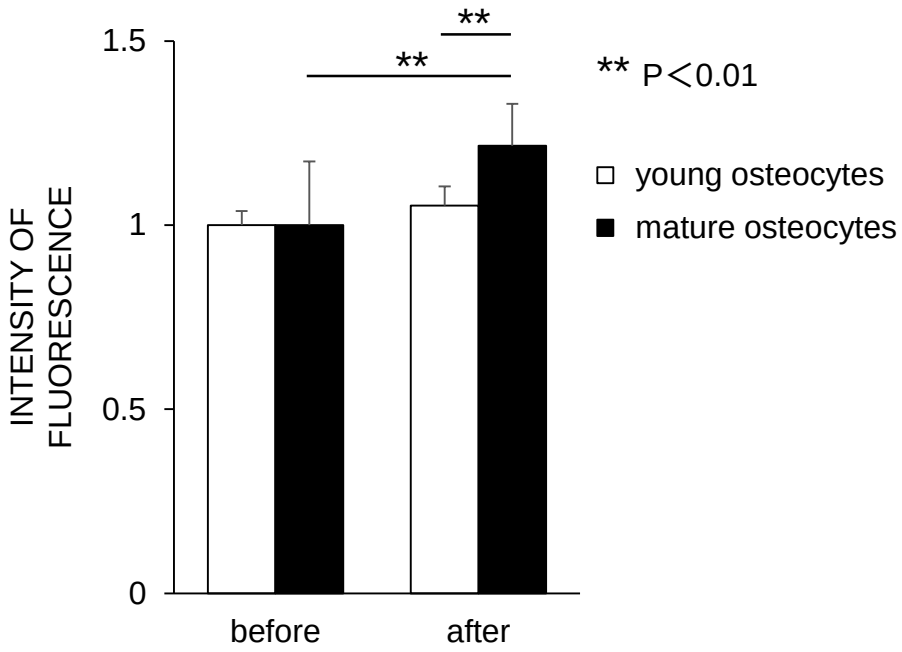

Fig. 2

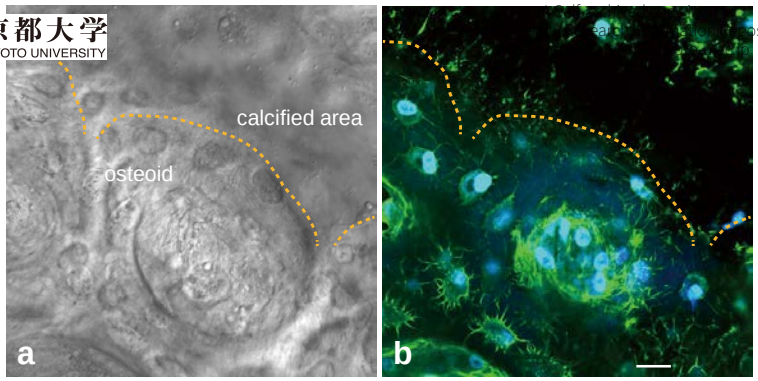

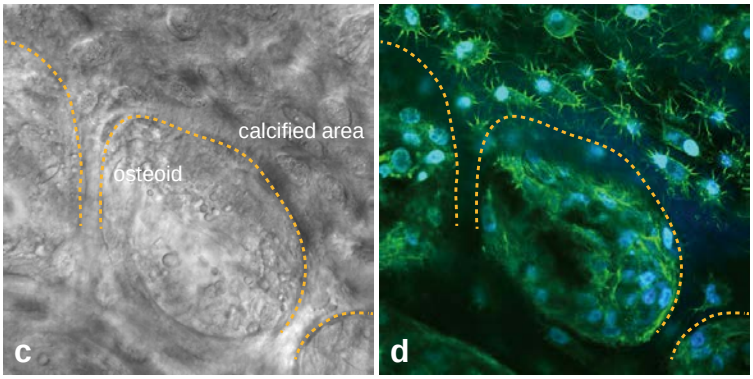

Bar=20μm

e

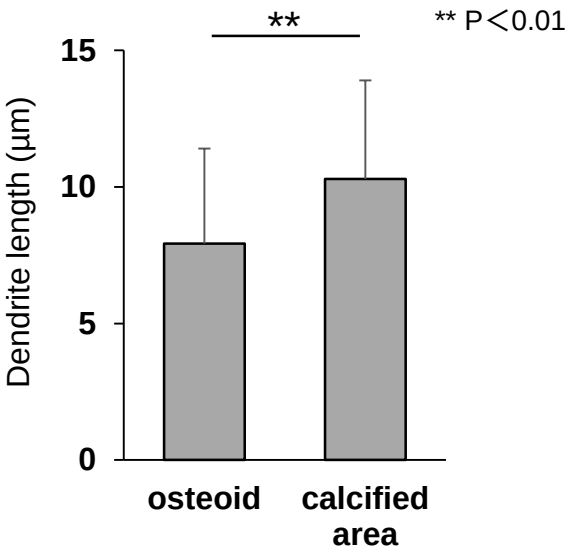

Fig. 3

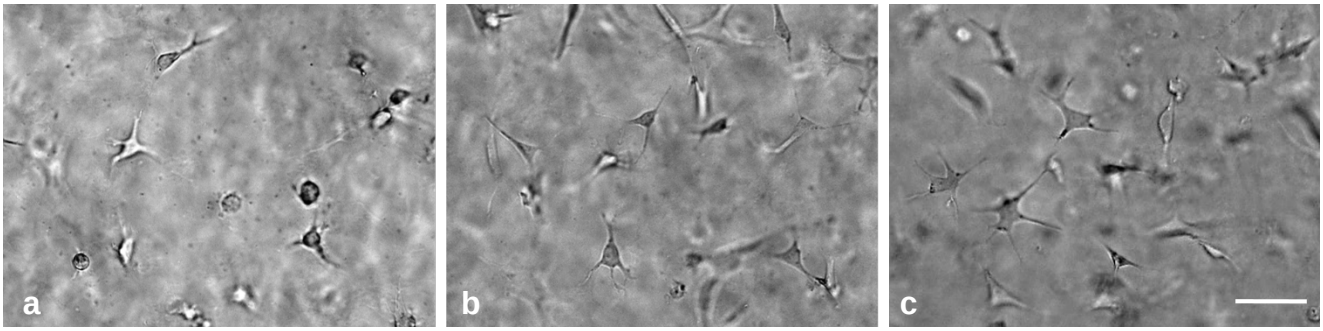

Bar=50μm

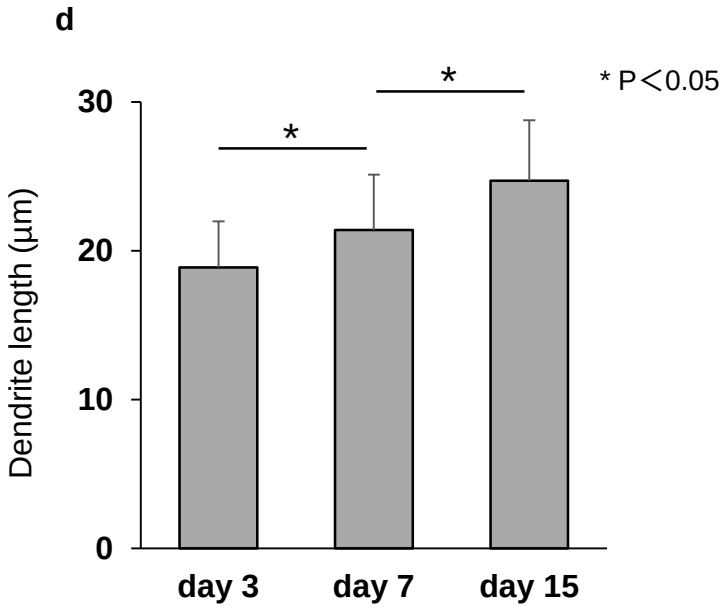

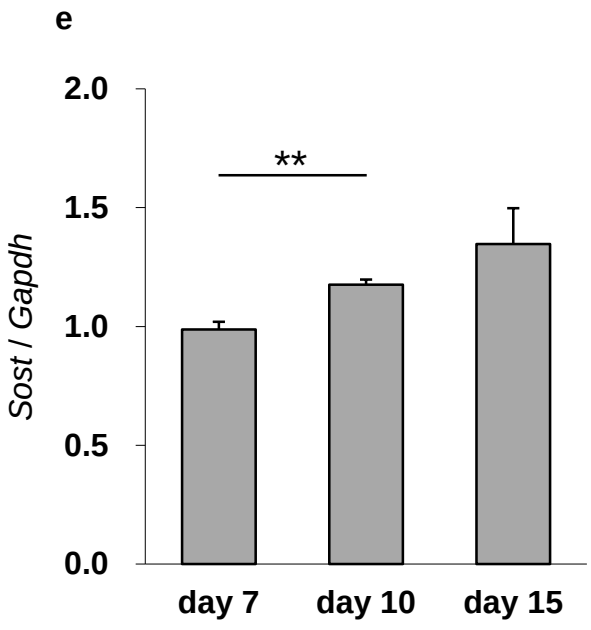

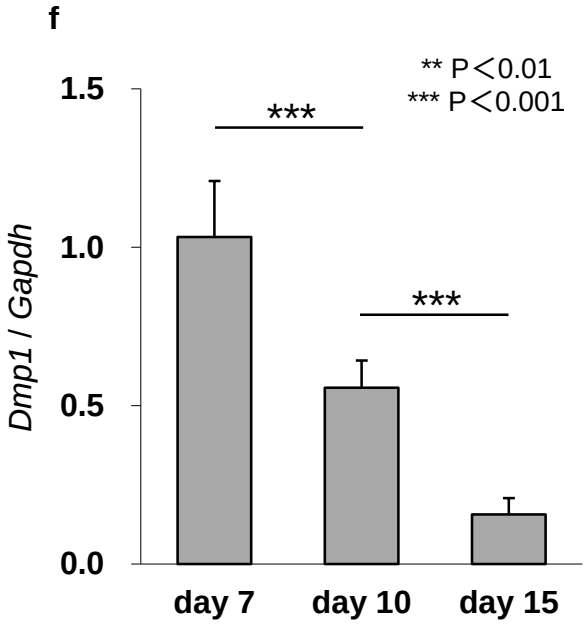

Fig. 4

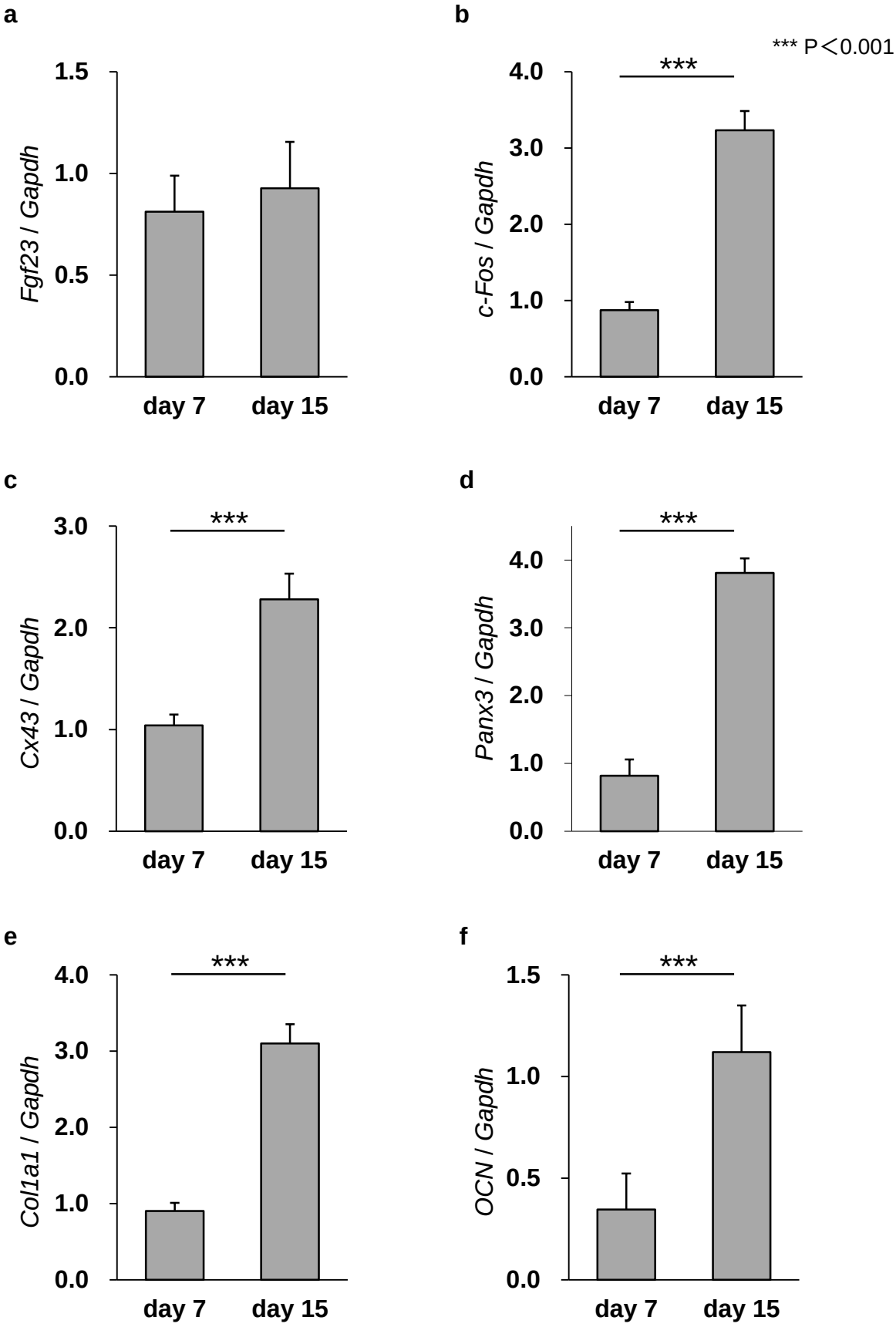

Fig. 5

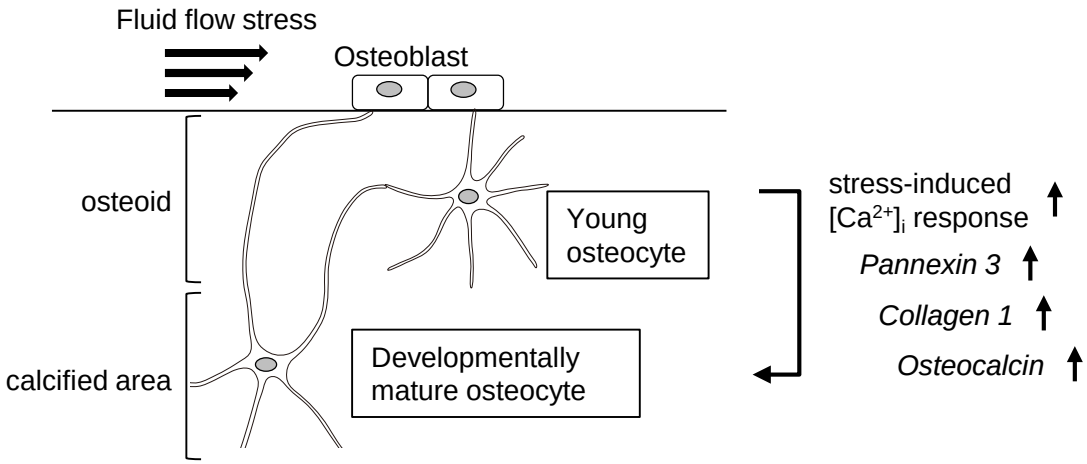

Fig. 6